CORROSION SCIENCE AND TECHNOLOGY, Vol.4, No.6(2005), pp.226~230

Effect of Si Addition on the Corrosion Resistance of Diamond-Like Carbon (DLC) Films

† Woo-Jung Kim[1], Jung-Gu Kim[1], Se-Jun Park[2], and Kwang-Ryeol Lee[2]

[1]Department of Advanced Materials Engineering, Sungkyunkwan University, 300 Chunchun-Dong, Jangan-Gu, Suwon 440-746, Korea
[2]Future Technology Research Division, Korea Institute of Science and Technology, P.O. Box 131, Cheongryang, Sungbuk-Gu, Seoul 130-650, Korea

Si incorporated diamond-like carbon (Si-DLC) films ranging from 0 to 2 at.% contents were deposited on STS 316L substrates for orthopedic implants by means of r.f. plasma-assisted chemical vapor deposition (r.f. PACVD) technique, using mixtures of benzene (C_6H_6) and silane (SiH_4) as the precursor gases. This study provides the reliable and quantitative data for assessment of the effect of Si incorporation on corrosion property in the simulated body fluid environment through the electrochemical test. It was found that corrosion to resistance of Si-DLC coatings with increasing Si content are improved owing to high sp^3 bonding.

Keywords : *Diamond-like carbon, Corrosion, EIS*

1. Introduction

In a method to improve resistance to wear and corrosion of protective coating, diamond-like carbon (DLC) coatings have been extensively studied over the past several years due to their unique properties. Especially, Si incorporated diamond-like carbon (Si-DLC) coatings have been attracting increased interest of researchers since they have a great potential for solving some of the major disadvantages of pure DLC coatings.[1)-4)] Moreover, the Si addition improved surface roughness and adhesion strength; therefore, improved surface roughness and adhesion strength could diminish production of pores. This is because the Si addition has a beneficial effect of promoting surface nucleation.[5)] Because of the remarkable collection of superior properties, many authors have noted the potential of Si-DLC coatings as a protective coating for orthopedic implants.

In this paper, we investigated that the effect of Si incorporation on corrosion properties of the Si-DLC coatings as a function of varying Si content deposited on 316 L stainless steel substrate with Si interlayer using electrochemical techniques.

† Corresponding author: kimjg@skku.ac.kr

2. Experimental procedure

2.1 Sample preparation

316L stainless steel was used as substrate materials. Samples of 37 mm diameter 316L stainless steel were cut from 2 mm thick sheet. Si-DLC coatings were deposited on mirror-polished substrate and Si-wafer. The sample surfaces were mechanically polished using 2000-grit SiC and 0.3 ㎛ diamond paste for the final step. After cleaning with TCE-aceton-methanol in ultrasonic cleaner sequentially, the polished samples were stored under vacuum. Details of the deposition equipment were previously described elsewhere.[6)] A substrate was placed on the water-cooled cathode where 13.56 MHz r.f. power was delivered through the impedance-matching network.

In r.f. PACVD method, the vacuum chamber is pumped by a rotary pump and a turbo molecular pump to a base pressure of approximately 2.0×10^{-3} Pa prior to deposition Before deposition, substrates were precleaned using argon plasma for 15 min at the bias voltage of -400 V and the pressure of 0.5 Pa. The coatings were deposited at a bias voltage of -400 V deposition and pressure of 1.33 Pa. The precursor gas was used as benzene mixture of C_6H_6 and silane (SiH_4) for the Si-DLC coatings. The Si-DLC coatings were produced with three different Si contents (0 at.% , 1.0 at.%, 2.0 at.%). The composition of Si-DLC coatings was measured by Rutherford backscattering spectroscopy using a collimated $^4He^{2+}$ ion beam of 2 MeV

An amorphous Si interlayer of thickness approximately 5 nm is deposited onto the substrate prior to Si-DLC coating for the improvement of adhesion between the coating and substrate. A total coating thickness of about 1 ㎛ was achieved in all cases. The coating thickness was analyzed by alpha-step profilometer.

2.2 Coating properties

Raman spectra of the deposited coatings were obtained using Raman spectrometer. The scanning electron microscope investigations were used to examine the surface morphology of the coatings as well as the corroded surfaces of tested specimens. Surface roughness of coating was analyzed using AFM operated in the contact mode. A root-mean-square (RMS) roughness was measured on the surface of Si-DLC coating using atomic force spectroscopy (AFM). RMS roughness is a very simple measure of height profile roughness. The RMS roughness describes the fluctuations of surface heights around an average surface height and is the standard deviation.

2.3 Electrochemical test

Experiments were performed in a 0.89% NaCl solution, saturated with purified nitrogen gas. The impedance measurements were carried out at open circuit potential (OCP) with amplitude of 10 mV in the frequency range from 10 mHz to 10 kHz. The equivalent circuit was used to carry out the fitting of the experimental EIS spectra collected at various intervals within the exposure of 216 h.[7] EIS has been used to determine the amount of delamination and water uptake of coatings exposed to an electrolyte. Thus, the extent of delamination area (A_d) and volume fraction of water uptake (V) could be determined from experimental values of pore resistance (R_{pore}) and coating capacitance (C_{coat}) obtained by the impedance diagrams on the basis of the equivalent circuit. The pore resistance (R_{pore}) of coating is related to the delamination area (A_d), i.e., the pore resistance (R_{pore}) decreases as the delaminated area increases. Therefore, delamination area (A_d) and volume fraction of water uptake (V) available within the coating were calculated by the following equations:

$$A_d = \frac{R^o_{pore}}{R_{pore}} \quad (1)$$

$$R^o_{pore} = \rho \times d(ohm \cdot cm^2) \quad (2)$$

$$V = \frac{\log\left[C_{coat}(t) / C_{coat}(0)\right]}{\log 80} \quad (3)$$

where R^o_{pore} was characteristic value for the corrosion reaction at the solution-coating interface, d coating thickness, ρ the coating resistivity, $C_{coat}(t)$ the coating capacitance as a function of time (t) and C_{coat} (0) the initial coating capacitance obtained from EIS data at initial exposure.

3. Results and discussion

3.1 Coating properties

The bonding structure of Si-DLC coatings was examined using the Raman spectroscopy, which is a powerful method for analyzing DLC coating due to its ability to distinguish between different bonding structures. Bonding ratio (sp^3/sp^2) of 0.98 for Si-DLC coating (0 at.%), 1.00 for Si-DLC coating (1.0 at.%) and 1.37 for Si-DLC coating (2.0 at.%), as shown in Fig. 1. This means that bonding ratio (sp^3/sp^2) of Si-DLC coatings with increasing Si content is increased. It is important that electrochemical properties were affected by bonding ratio (sp^3/sp^2) of coating.

The surface morphology of Si-DLC coatings with increasing Si content indicated smaller pitting area and evidence of less amount penetration of water and ions, as shown in Fig. 2. This clearly indicates that Si-DLC coatings with increasing Si content have excellent corrosion resistance. The coating surface roughness of 0.0906 ㎛ for Si-DLC coating (2.0 at.%), 0.1178 ㎛ for Si-DLC coating (1.0 at.%) and 0.2326 ㎛ for Si-DLC coating (0 at.%) was examined through the AFM measurements. This surface roughness is caused by the craters and surface flaws distributed in the outer surface of coating. Thus, the surface becomes smoother and defects vanish with increasing Si content.

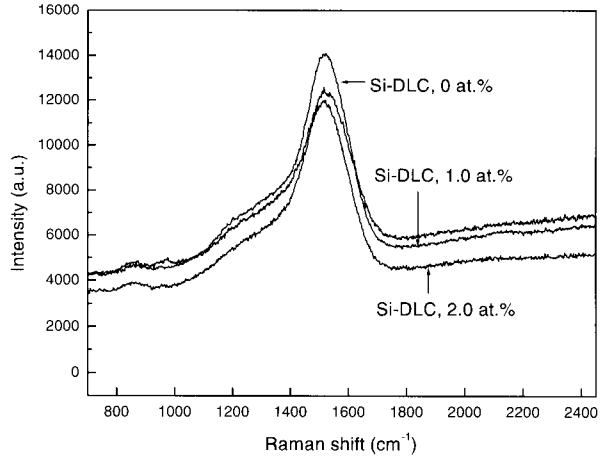

Fig. 1. Raman spectra of Si-DLC coatings deposited at different Si content.

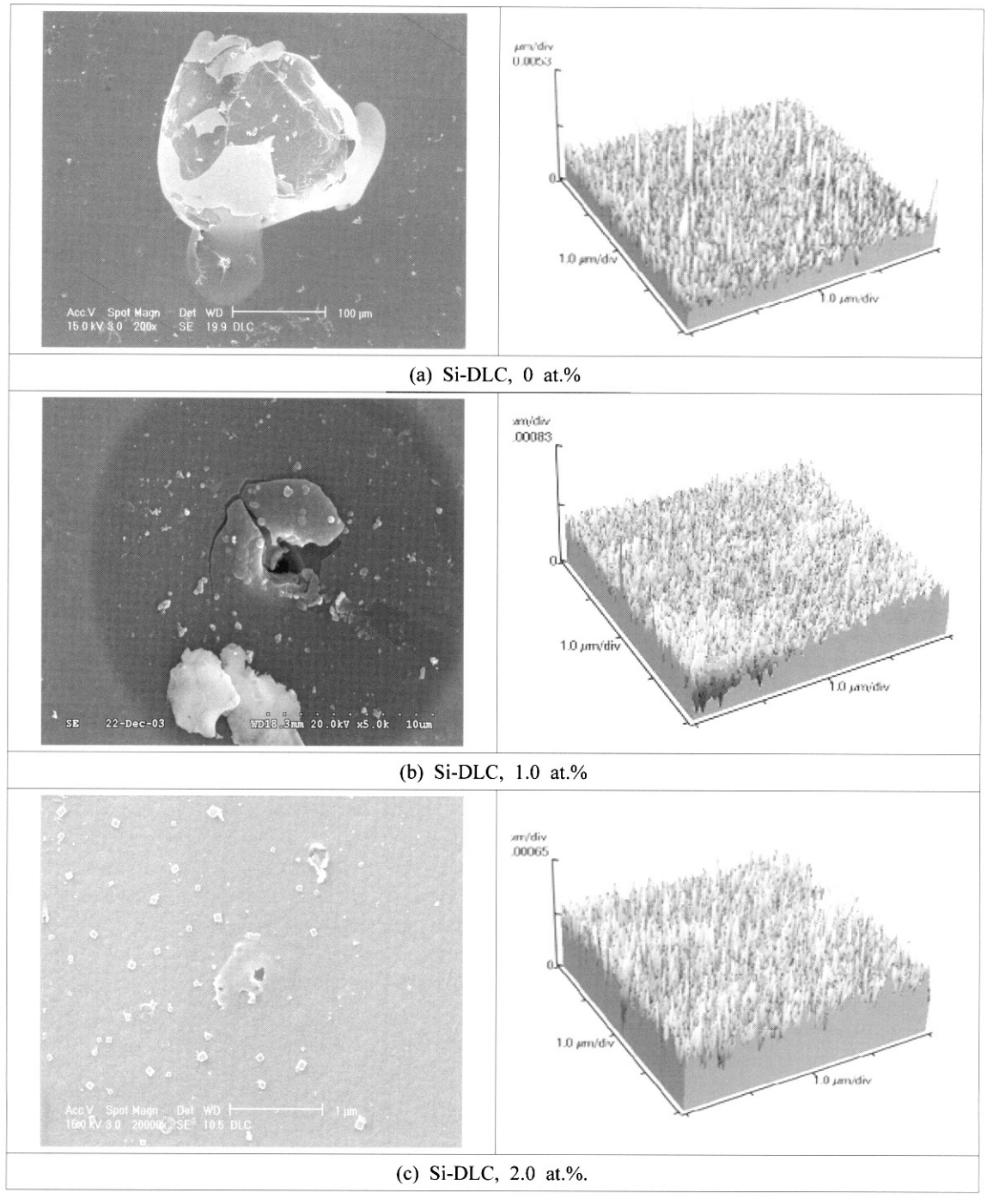

Fig. 2. SEM and AFM images of Si-DLC coatings.

3.2 Electrochemical properties

Interpretation of the EIS measurements is usually done by fitting the impedance data to an equivalent circuit, which is representative of the physical processes taking place in the system under investigation. The results obtained from EIS measurements through equivalent circuit were usually used to monitor the change of delamination area (A_d) and volume fraction of water uptake (V).[8] After a variable change of delamination area during the 96 h immersion, Si-DLC coatings showed a slight increase or an invariable fluctuation, as shown in Fig. 3. Delamination area was affected by the volume fraction of water uptake through porous coating because penetration of water in coating led to delamination and blisters. It is seen that

longer times of exposure lead to a continuous increase of the volume fraction of water uptake. Especially, the volume fraction of water uptake of Si-DLC coating (0 at.%) tends to absorb more water due to the enhancement of diffusion mechanisms of active species through the coating. These imply that water and ions first saturates the coating and then ionic species penetrate through the defects of the coating and gradually saturate the substrate surface. Consequently, the delamination area and volume fraction of water uptake of Si-DLC coatings with increasing Si content are much lower than those of Si-DLC coating (0 at.%), as shown in Table 1 and Figs. 3 and 4. These mean that delamination area and volume fraction of water uptake with increasing Si content absorb less

Table 1. Result of electrochemical impedance spectroscopy measurements.

Exposure time		R_s (Ω cm^2)	CPE1		R_{pore} ($*10^3$ Ω cm^2)	CPE2		R_{ct} ($*10^3$ Ω cm^2)	A_d ($*10^{-4}$)	V
			C_{coat} ($*10^{-9}$ F/cm^2)	n (0-1)		C_{dl} ($*10^{-9}$ F/cm^2)	n (0-1)			
120h	Substrate	32.96	46440	1	78.99	175200	1	252.2	-	-
	Si-DLC (0 at.%)	929.1	878.4	0.6016	92.48	714.2	1	372.5	1.78	3.15
	Si-DLC (1.0 at.%)	424.5	442.4	0.8999	95.2	532.4	1	627	1.51	3.00
	Si-DLC (2.0 at.%)	700.7	20.83	0.9921	3.433	47.47	0.7483	2501	0.41	1.91
168h	Substrate	34.57	47980	1	76.53	169400	1	230.2	-	-
	Si-DLC (0 at.%)	719.8	892.4	0.6017	89.99	120.6	1	387.8	1.83	3.16
	Si-DLC (1.0 at.%)	321.9	445.7	0.8743	93.9	535.4	1	497	1.53	3.01
	Si-DLC (2.0 at.%)	882.4	26.4	1	3.175	43	0.7375	3566	0.45	1.96
216h	Substrate	33.29	48210	1	73.42	174200	1	218.2	-	-
	Si-DLC (0 at.%)	696	899.4	0.6099	89.01	542.2	1	342	1.83	3.16
	Si-DLC (1.0 at.%)	297.6	474.2	0.8765	92.7	541.4	1	469	1.55	3.02
	Si-DLC (2.0 at.%)	4.308	27.12	0.9602	2.95	47.05	0.5329	2062	0.48	1.97

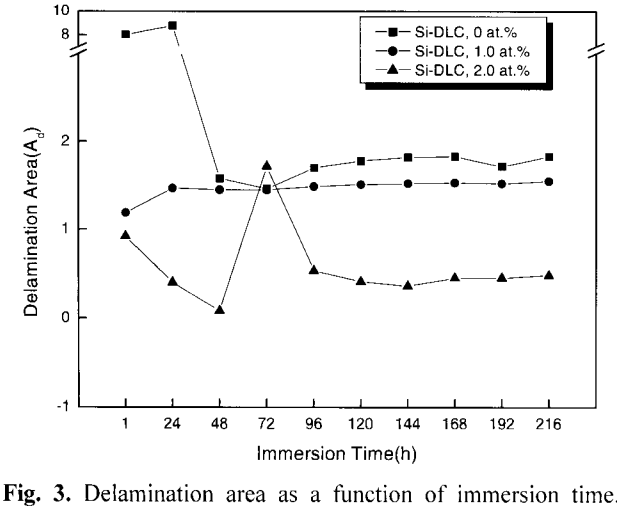

Fig. 3. Delamination area as a function of immersion time.

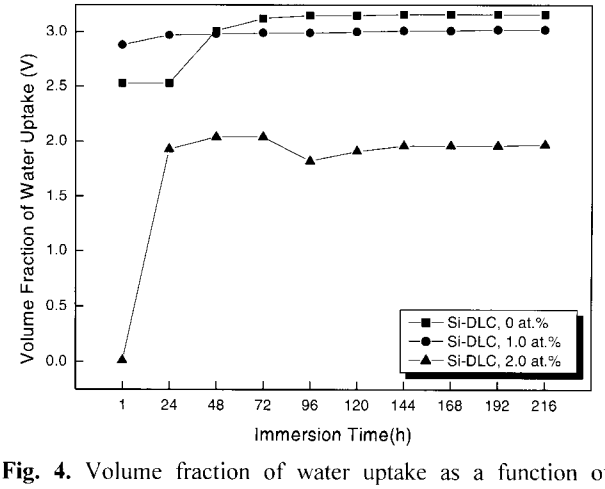

Fig. 4. Volume fraction of water uptake as a function of immersion time.

amount of water compared to Si-DLC coating (0 at.%). Furthermore, this implies that increasing of Si content led to an increase in the dense sp^3 bonding and a decrease in the percentage and dimensions of those defects like pinhole and damage zone, etc. Xu et al. have also shown that higher bonding ratio (sp^3/sp^2) enhanced the corrosion resistance.[9] The excellent agreement between the delamination area and the volume fraction of water uptake over the test period suggests that porosity is indeed strongly related to the coating delamination and the volume fraction of water uptake which is wetted by the electrolyte through defects.

4. Conclusions

1) An increase of bonding ratio (sp^3/sp^2) with increasing Si content indicated improved corrosion resistance.

2) From the SEM and AFM images, the pitting corrosion of Si-DLC coatings with an increase of Si content was not as severe as those of Si-DLC coating (0 at.%), and the surface becomes smoother and defects vanish with increasing Si content.

3) An increase of Si content reduced delamination area (A_d) and volume fraction of water uptake (V) in Si-DLC coatings.

Acknowledgments

The authors are grateful for the support provided by the Korea Science and Engineering Foundation through the Center for Advanced Plasma Surface Technology at Sungkyunkwan University.

References

1. J. C. Damasceno, S. S. Camargo Jr, F. L. Freire Jr, R. Carius, *Surface and Coating Technology,* **133**, 247 (2000).
2. T. Ohana, T. Nakamura, M. Suzuki, A. Tanaka, and Y. Koga, *Diamond and Related Materials,* **13**, 1500 (2004).
3. A. A. Ogwu, T. Coyle, T. I. T. Okpalugo, P. Kearney, P. D. Maguire, and J. A. D. McLaughlin, *Acta Materialia,* **51**, 3455 (2003).
4. C. Fernández-Ramos, J. C. Sánchez-López, M. Belin, C. Donnet, L. Ponsonnet, and A. Fernández, *Diamond and Related Materials,* **11**, 169 (2002).
5. P. Papakonstantinou, J. F Zhao, P. Lemoine, E. T. McAdams, and J. A. McLaughlin, *Diamond and Related Materials,* **11**, 1074 (2002).
6. J. G. Kim, Z. T. Park, J. H. Yoo, and W. S. Hwang, *Corrsion Science and Technology,* **3**, 118 (2004).
7. Y. Umehara, et al, *Diamond and Related Materials,* **11**, 1429 (2002).
8. W. I. Urruchi, *Diamond and Related Materials,* **9**, 685 (1993).
9. H. Liu and D. S. Dandy, *Diamond Chemical Vapor Deposition*, Noyes Publications, USA, New Jersey, pp. 44 (1995).